Exploration of Shear Stresses Induced by a Contrast Agent Bubble on the Cell Membrane

Alexander A. Doinikov, Ayache Bouakaz

10eme Congres Francais d'Acoustique
Lyon, 12-16 Avril 2010

Exploration of shear stresses induced by a contrast agent bubble on the cell membrane

Alexander Doinikov[1,2], Ayache Bouakaz[1]

[1]INSERM U930 CNRS ERL3106, Universite Francois Rabelais, CHU Bretonneau, 2 Boulevard Tonnelle, 37044 Tours Cedex 09, doinikov@bsu.by
[2]LE STUDIUM®, Institute for Advanced Studies, Orleans and Tours

The subject of this study is shear stress exerted on the cell membrane by acoustic microstreaming generated by a contrast microbubble pulsating nearby a cell. This effect is presumed to play a major role in the sonoporation process. Currently, the existing model of this effect is based on an equation that has been derived for a free hemispherical bubble resting on a rigid plane. Such a model is not adequate for an encapsulated bubble such as a contrast agent microbubble. In this study, an improved theory is suggested that assumes an encapsulated bubble to be detached from the cell membrane. The new model allows one to calculate the shear stress distribution on the cell membrane and to determine the position and the magnitude of the peak shear stress at different values of the acoustic parameters. The second problem under consideration is how to apply the model for pairwise bubble-cell interactions to bubble-cell solutions which one has to deal with in experiments. An approach is proposed to evaluate the number of cells undergoing sonoporation in a bubble-cell solution. It is shown that the reaction of a bubble-cell solution to the variation of the acoustic parameters can be different from what is expected from the analysis of pairwise interactions between single bubbles and cells. In particular, the attenuation of the driving acoustic wave caused by bubbles can considerably reduce the total efficiency of sonoporation in the solution at frequencies close to the resonance frequency of bubbles of dominant size. Numerical examples for a polydisperse bubble population are presented.

1 Introduction

In recent years new promising possibilities for targeted drug and gene delivery have been discovered that can be realized by using ultrasound contrast agents. Ultrasound contrast agents are micron-sized encapsulated gas bubbles which are produced by pharmaceutical companies for medical ultrasound applications [1]. The encapsulation is necessary to prevent bubbles from fast dissolution in blood and coalescence. Initially, contrast agents were used in ultrasonic diagnostics. In this case, they are injected into the bloodstream of the patient in order to increase the contrast between blood and tissue during an ultrasonic examination and thereby to improve the quality of ultrasonic images and diagnosis confidence. More recently, specific contrast agents have been designed that are capable of selectively adhering to desired target sites in the human body [2]. Moreover, such targeted contrast agents can carry drugs or genes inside or on the encapsulating shell. This capability, in combination with the phenomenon known as sonoporation, provides unprecedented possibilities for a highly selective therapeutic action. The term "sonoporation" denotes a process in which ultrasonically activated contract microbubbles, pulsating nearby cells, increase the permeability of cell membranes and thereby enhance the penetration of external substances into cells [3]. In this way drugs and genes can be delivered inside individual cells without serious consequences for the cell viability. In spite of numerous experimental investigations on sonoporation, the mechanism of this phenomenon remains unknown. The dominant hypothesis is currently that the penetration of foreign molecules from the extracellular space occurs through transient micropores in the cell membrane [4-6]. The pores are supposed to arise in response to shear stresses that are exerted on the cell membrane by acoustic microstreaming generated by a contrast microbubble when it is pulsating nearby a cell. This process is depicted schematically in Fig. 1.

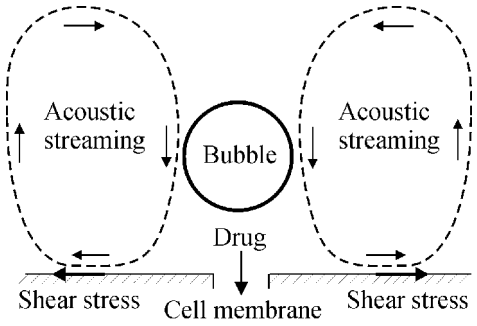

Figure 1 : Schematic sketch of the sonoporation process.

To estimate the shear stress created on the cell membrane, a formula is used that was adopted from the theory developed by Nyborg [7] in the context of ultrasound cavitation cleaning. This formula was derived for a gas hemisphere resting on a rigid infinite plane. It is evident that such a model is not adequate for an encapsulated bubble. Therefore the first purpose of the present study was to develop a more correct model, assuming that a contrast bubble is detached from the cell membrane. The second problem considered is how to apply the model for pairwise bubble-cell interactions to bubble-cell solutions which one has to deal with in experiments. In particular, it is known that, as the driving ultrasonic wave propagates through a bubble-cell solution, it is attenuated because of the scattering by contrast microbubbles. As a result, microbubbles are exited at different acoustic pressure

amplitudes depending on their position inside the solution, which affects their possibility to produce stresses necessary for sonoporation. In the present paper, an approach is proposed that allows one to evaluate the number of sonoporated cells in a bubble-cell solution, taking into account the attenuation of the imposed ultrasound field.

2 Theoretical model for pairwise bubble-cell interactions

Nyborg [7] developed an approximate method for calculating acoustically-induced steady vortical flow near a fluid-solid interface. This flow, referred to as acoustic streaming, occurs near the surfaces of obstacles and vibrating objects in a viscous fluid subject to an acoustic wave field. Nyborg's theory allows one to estimate shear stresses produced on a rigid boundary by acoustic microstreaming that is generated by a small sound source situated in the vicinity of the boundary. To apply Nyborg's theory to a specific sound source, it is necessary at first to calculate the irrotational oscillatory velocity field that is generated by the sound source near the boundary assuming that the ambient liquid is nonviscous. As an example, Nyborg applied his theory to the case of a pulsating gas hemispherical bubble resting on a rigid plane. In this case, according to his results, the maximal shear stress exerted on the plane can be represented as

$$\tau_{\max} = 0.5\left(\rho_L \eta_L / \pi f\right)^{1/2} U_m^2 / R_0 , \qquad (1)$$

where ρ_L and η_L are the equilibrium density and viscosity of the ambient liquid, f is the driving frequency, U_m is the maximum during an acoustic cycle of the radial velocity of the bubble wall, and R_0 is the equilibrium radius of the bubble. Rooney [8] expressed (1) in terms of the displacement amplitude of the bubble wall, denoted below by ξ_m, and obtained the following formula:

$$\tau_{\max} = 2(\rho_L \eta_L)^{1/2} \left(\pi f\right)^{3/2} \xi_m^2 / R_0 . \qquad (2)$$

Rooney believed that in this formulation Nyborg's result can be applied to sound sources other than a pulsating hemispherical bubble, such as a vibrating Mason horn.

Lewin and Bjorno [9] suggested using the Rayleigh-Plesset equation to calculate ξ_m. Later on, Wu [10] assumed that (2) can be applied to an encapsulated bubble by using a modified Rayleigh-Plesset equation that accounts for encapsulation,

$$R\ddot{R} + \frac{3}{2}\dot{R}^2 = \frac{1}{\rho_L}\left[P_{g0}\left(\frac{R_0}{R}\right)^{3\gamma} - \frac{2\sigma}{R} - \frac{4\eta_L \dot{R}}{R} - P_0 - P_{ac}(t) - S \right]. \qquad (3)$$

Here $R(t)$ is the instantaneous bubble radius, the overdot denotes the time derivative, P_{g0} is the equilibrium gas pressure within the bubble, γ is the ratio of specific heats of the gas, σ is the surface tension, P_0 is the hydrostatic pressure, and $P_{ac}(t)$ is the driving acoustic pressure. The effect of encapsulation is described by the term S, which was taken by Wu in the form suggested by de Jong *et al.* [11]. Since then this theory has been used to estimate shear stresses produced by a contrast bubble on the cell membrane [12].

Clearly, however, that for an encapsulated bubble the assumption underlying Nyborg's formula (2) is not appropriate. A more suitable assumption would be that a contrast bubble oscillates near a cell, being detached from the cell membrane. This situation is depicted in Fig. 2, where d denotes the distance between the center of the bubble and the cell membrane. The dashed circle represents

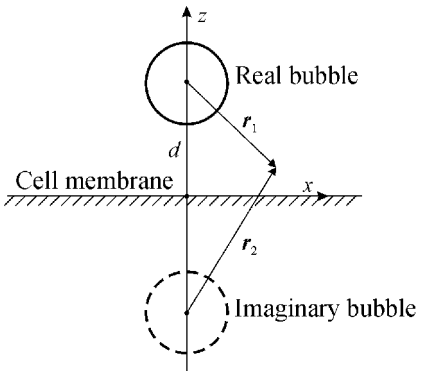

Figure 2 : An encapsulated bubble near the cell membrane.

an imaginary bubble that is required to satisfy the boundary conditions on the cell membrane. We will assume that the cell membrane behaves as a rigid plane. In this case, the necessary boundary conditions are satisfied by assuming that both bubbles are equal, pulsating in phase, and the plane is halfway between them. Reasons for the approximation of the cell membrane as a rigid plane are discussed in Section 4.

For the situation shown in Fig. 2, (3) is not valid as it was derived for a bubble in an unbounded liquid. To take into account the presence of a rigid plane, (3) is modified by introducing an additional term as proposed in [13],

$$R\ddot{R} + \frac{3}{2}\dot{R}^2 = \frac{1}{\rho_L}\left[P_{g0}\left(\frac{R_0}{R}\right)^{3\gamma} - \frac{2\sigma}{R} - \frac{4\eta_L \dot{R}}{R} - P_0 - P_{ac}(t) - S \right] - \left(R\ddot{R} + 2\dot{R}^2\right) R / 2d . \qquad (4)$$

The next step is to obtain a refined formula for shear stress instead of (2). In view of the cylindrical symmetry of the problem considered, there is no loss in generality if the consideration is restricted to the xz plane as shown in Fig. 2. Then the irrotational liquid velocity that is generated in the situation shown in Fig. 2 can be written as

$$\boldsymbol{u} = \left(\boldsymbol{r}_1 / r_1^3 + \boldsymbol{r}_2 / r_2^3\right) \dot{R} R^2 , \qquad (5)$$

where

$$\boldsymbol{r}_1 = x\boldsymbol{e}_x + (z-d)\boldsymbol{e}_z , \quad \boldsymbol{r}_2 = x\boldsymbol{e}_x + (z+d)\boldsymbol{e}_z . \qquad (6)$$

Following Nyborg's approach, we linearize (5) setting $R = R_0$ and $dR/dt = i\omega\xi_m \exp(i\omega t)$, where $\omega = 2\pi f$. As a result, the amplitude of the x component of the velocity $\boldsymbol{u}$ is written as

$$u_{x0} = \frac{2\pi f \xi_m R_0^2 x}{\left[x^2 + (z-d)^2\right]^{3/2}} + \frac{2\pi f \xi_m R_0^2 x}{\left[x^2 + (z+d)^2\right]^{3/2}} . \qquad (7)$$

For the case under consideration, the shear stress produced on the plane (cell membrane) shown in Fig. 2 is given by Nyborg's theory to be

$$\tau_x = 0.25\left(\rho_L \eta_L / \pi f\right)^{1/2} \left(u_{x0} \partial u_{x0} / \partial x\right)_{z=0} . \qquad (8)$$

Substitution of (7) into (8) yields

$$\tau_x = 4(\rho_L \eta_L)^{1/2} \left(\pi f\right)^{3/2} \frac{\xi_m^2}{R_0} \left(\frac{R_0}{d}\right)^5 \frac{\beta - 2\beta^3}{(1+\beta^2)^4} , \qquad (9)$$

where $\beta = x/d$. The β-dependent factor on the right-hand side of (9) has a maximum at $\beta_{\max} = \sqrt{(13-\sqrt{129})/20}$. It is seen that the shear stress increases as d decreases and the maximum stress is reached when the microbubble is in contact with the plane (cell membrane). The maximum value of the shear stress in the x direction (on the cell membrane) takes place along a circle whose center is the projection of the center of the microbubble on the plane, and the radius of the circle is equal to $\beta_{\max} d$ when the microbubble is at distance d from the plane.

Let us consider the shear stress distribution that is created by a contrast microbubble on the cell membrane in accord with (4) and (9). An example of such a distribution is shown in Fig. 3. In this calculation, the shell model suggested in [14] has been used,

$$S = 4\chi\left(\frac{1}{R_0}-\frac{1}{R}\right) + 4\left|\frac{\kappa_0}{1+\lambda\,|\dot{R}|/R}+\kappa_1\frac{\dot{R}}{R}\right|\frac{\dot{R}}{R^2}, \qquad (10)$$

where χ is the shell surface elastic modulus, κ_0 and κ_1 are parameters describing the viscous behavior of the shell, and the normalizing factor $\lambda = 4$ μs. The shear stress distribution shown in Fig. 3 was calculated for a contrast microbubble with the initial radius $R_0 = 1.5$ μm at $d = 2\,R_0$, $f = 2.0$ MHz, and the acoustic pressure amplitude $P_{m0} = 200$ kPa. The other parameters used in this calculation were the following: $P_0 = 101.3$ kPa, $\rho_L = 1000$ kg/m^3, $\eta_L = 0.001$ Pa·s, $c = 1500$ m/s, $\gamma = 1.07$, $\sigma = 0.072$ N/m, $\kappa_0 = 1.2\ 10^{-7}$ kg/s, $\kappa_1 = 2.0\ 10^{-15}$ kg , and $\chi = 0.12$ N/m.

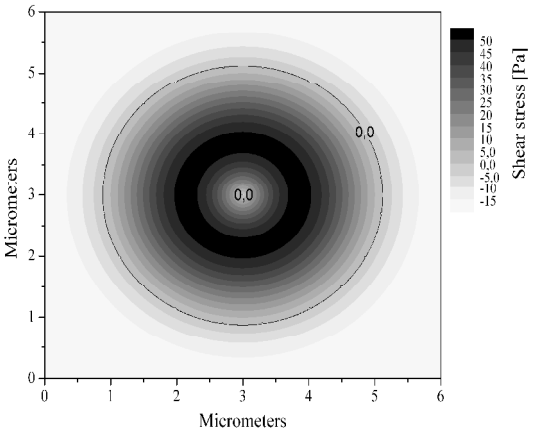

Figure 3 : Shear stress distribution created by a contrast microbubble on the cell membrane.

The central point 0.0 in Fig. 3 is straight under the center of the bubble. Positive values of shear stress in Fig. 3 mean that the stress is directed away from the central point, and vice versa. Figure 3 shows that at the point which is the projection of the bubble center on the cell surface, the shear stress is zero, then it increases, being directed away from the bubble, reaches a maximum (the darkest area), decreases down to zero (the black circle with the label 0.0), and changes sign, getting directed to the bubble. The reason of zero stress at the center is that at this point shear stresses act in all directions and therefore compensate each other. It is this point that is the site of a possible rupture.

The shear stress distribution shown in Fig. 3 predicts the following pattern of the behavior of the cell membrane. When the imposed acoustic pressure reaches a threshold value, a rupture emerges at the central point. The stretching shear stresses widen the emerged hole until the counteraction of the cell membrane stops this process. When the ultrasound is off, the hole closes due to the back reaction of the cell membrane. This is the case of non-lethal sonoporation. If, however, the imposed acoustic pressure is strong so that the expansion of the hole damages irreversibly the structure of the cell membrane, then the hole doest not vanish completely after ultrasound exposure. This is the case of lethal sonoporation.

3 Modeling of sonoporation in a bubble-cell solution

In experiments one has to deal with bubble-cell solutions. Therefore the question arises as to how to compare measurements made for a bubble-cell solution with the theory for pairwise bubble-cell interactions.

Let us assume that a bubble-cell solution under investigation occupies a container with depth D and cross-section area A. As the driving acoustic wave propagates through the container, it is attenuated because of the presence of contrast microbubbles. As a result, the microbubbles are excited at different acoustic pressure amplitudes depending on their position in the container. This process can be described as follows.

The acoustic wave field can be represented as

$$P_{ac}(t) = P_{m0}\exp(i\omega t - ikz), \qquad (11)$$

where z denotes the direction of the wave propagation toward the interior of the container and k is the wave number that takes into account the presence of microbubbles. The attenuation coefficient is then defined as α = -Im$\{k\}$ and the acoustic pressure amplitude at the distance z deep into the container is given by

$$P_m = P_{m0}\exp(-\alpha z). \qquad (12)$$

Substituting (11) into (4), one can calculate ξ_m for a contrast bubble with radius R_0 located at depth z, and then, substituting ξ_m into (9), one can calculate the shear stress produced by this bubble.

Let us now assume that there is a threshold value of shear stress which, when being experienced by the cell membrane, leads to the onset of sonoporation. In the literature, a value of 12 Pa is reported [10]. Using (4), (9), and (11), one can calculate the critical depth z_{cr} at which the maximum shear stress generated by a bubble with radius R_0 drops below the threshold shear stress τ_{cr} necessary for sonoporation.

To go on with the derivation, one has to make simplifying assumptions. Let us assume that (a) cells and bubbles are uniformly distributed within the container, (b) the number of bubbles is equal to that of cells, (c) the specific bubble concentration is low enough to ignore bubble-bubble interactions, (d) bubbles are in the immediate vicinity of cells, and (e) there is only one bubble beside each cell. The first three conditions can be satisfied by proper preparation of a bubble-cell solution. The fourth condition can be obtained by means of preliminary insonification of the bubble-cell solution with relatively weak ultrasound. As a result, secondary acoustic radiation forces should bring together bubbles and cells. The fifth condition cannot be created by intent, but statistically, one can expect that such situations dominate the solution and

hence their contribution will be dominant as well. It should be also mentioned that strong ultrasound can give rise to global liquid motions in the container, such as large-scale acoustic streaming. The complexity of such processes makes it difficult to determine the degree of their influence on the process of sonoporation and to point out the way by which this influence could be taken into account. Therefore special experimental preparations should be made to minimize such processes.

Under the conditions pointed out above, the number of sonoporated cells in the container can be evaluated as

$$N_{sc} = A \int_{R_{\min}}^{R_{\max}} z_s(R_0) n_b(R_0) dR_0 , \qquad (13)$$

where $n_b(R_0)$ is the distribution function of contrast bubbles over radii so that $n_b(R_0)dR_0$ is the number of bubbles with radii from R_0 to $R_0 + dR_0$ per unit volume. Note that (13) gives the number of cells undergoing both reparable and lethal sonoporation. The total number of cells in the container is given by $N_c = ADn_c$, where n_c is the number of cells per unit volume, which, by assumption, is equal to the number of bubbles per unit volume, that is,

$$n_c = \int_{R_{\min}}^{R_{\max}} n_b(R_0) dR_0 . \qquad (14)$$

It follows that the percentage of sonoporated cells can be evaluated as

$$P_{sc} = \frac{\int_{R_{\min}}^{R_{\max}} z_{cr}(R_0) n_b(R_0) dR_0}{D \int_{R_{\min}}^{R_{\max}} n_b(R_0) dR_0} . \qquad (15)$$

The problem remains as to how to evaluate the wave number k in the case of nonlinear oscillations. The following method can be proposed. The wave number in a bubbly liquid can be expressed in terms of the amplitude of the bubble oscillation as [15]

$$k = \frac{\omega}{c} - \frac{2\pi\omega\rho_L c}{P_{m0}} \times \int_{R_{\min}}^{R_{\max}} \xi_{m0} \exp(-i\varphi) R_0^2 n_b(R_0) dR_0 , \qquad (16)$$

where c is the speed of sound in the ambient liquid, ξ_{m0} is the amplitude of the oscillation of a bubble with radius R_0 at pressure P_{m0}, and φ is the phase delay of the bubble oscillation with respect to the driving pressure $P_{ac}(t)$. The quantities ξ_{m0} and φ can be calculated from (4) and substituted into (16). It should be noted, however, that (16) is derived from the linear equations of wave propagation. We assume that this equation is still valid for the cases considered here.

Figure 4 demonstrates an example of using (15) and (16) for the modeling of sonoporation processes in a bubble-cell solution. The percentage of sonoporated cells is depicted as a function of the driving frequency at different pressures. It is assumed that τ_{cr} = 12 Pa, D = 0.015 m, d = R_0, and the bubble size distribution function $n_b(R_0)$ corresponds to that of the contrast agent SonoVue (Bracco Research SA, Geneva, Switzerland) with the volume bubble concentration 10^{-5} ($3\ 10^5$ microbubbles per 1 ml). The other parameters used in this calculation were the following: P_0 = 101.3 kPa, ρ_L = 1000 kg/m^3, η_L = 0.001 Pa·s, c = 1500 m/s, γ = 1.07, and σ = 0.072 N/m. For a shell model, (10) was taken. It is known that all available shell models show that their shell parameters are dependent on the equilibrium bubble radius [14]. This fact should be taken into consideration when simulations for a polydisperse bubble population are performed. Based on the results of [14], the following linear regression equations for the best-fit values of the shell parameters of the model (10) were used:

$$\kappa_0(R_0) = 10^{-7}\left(0.28R_0 + 0.65\right), \qquad (17)$$

$$\kappa_1(R_0) = 10^{-15}\left(1.8R_0 - 1.1\right), \qquad (18)$$

$$\chi(R_0) = 0.28R_0 - 0.30 , \qquad (19)$$

where R_0 is specified in micrometers.

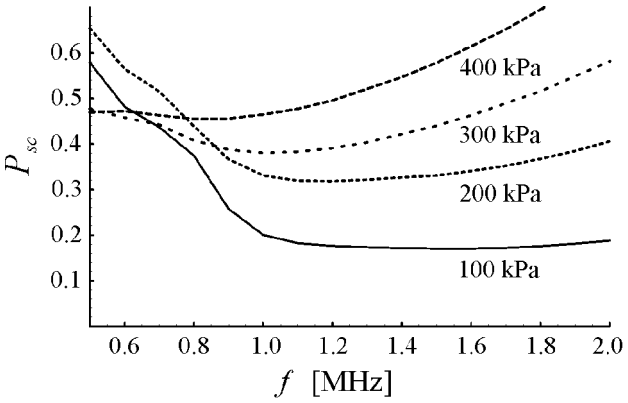

Figure 4 : Dependence of the percentage of sonoporated cells P_{sc} on the driving frequency at different values of the acoustic pressure amplitude P_{m0}.

Figure 4 suggests that the minimum of the sonoporation efficiency corresponds to the resonance frequency of contrast microbubbles of dominant size, since at this frequency the attenuation of the acoustic field becomes maximal. One can see that, if bubbles of dominant size are excited below their resonance frequency, the efficiency of sonoporation decreases as the driving frequency increases. Increasing the driving frequency may again lead to an increase in the efficiency of sonoporation only when bubbles of dominant size are excited well above their resonance frequency.

4 Conclusion

There are numerous experimental investigations on sonoporation, while the theoretical background of this phenomenon still is in its infancy. There are two main theoretical problems to be solved. The purpose of the first one is to study how the interaction between a cell and an ultrasound-induced contrast microbubble leads to sonoporation and to develop a simulation model for this interaction. The second problem is how to apply the above model of pairwise bubble-cell interactions to bubble-cell solutions which one has to deal with in experiments in order to compare theoretical predictions with experimental measurements. Both problems have been considered in this study.

At present the dominant opinion is that sonoporation is caused by shear stress exerted on the cell membrane by acoustic microstreaming generated by a contrast microbubble pulsating nearby a cell. However, the existing

model of this effect is based on an equation that has been derived for a gas hemisphere resting on a rigid plane. It is evident that such a model is not adequate for an encapsulated bubble such as a contrast agent microbubble. In this paper, an improved theory is suggested that assumes a contrast microbubble to be detached from the cell membrane. Simulations made by using the improved model have allowed one to calculate the shear stress distribution created on the cell membrane by an adjacent pulsating contrast microbubble. It has been shown that the maximum of the shear stress on the cell surface occurs along a circle whose radius is about $0.287d$, where d is the distance between the bubble and the cell. This maximum value is likely to determine the threshold value of shear stress which leads to the onset of sonoporation.

A method has been proposed as to how the model for pairwise interactions between bubbles and cells can be applied to a bubble-cell solution in order to evaluate the number of sonoporated cells at different values of the acoustic parameters. It has been shown that the attenuation of the driving acoustic wave caused by contrast microbubbles can considerably decrease the efficiency of sonoporation in a bubble-cell solution at frequencies close to the resonance frequency of bubbles of dominant size.

In conclusion, we would like to discuss the limitations of the theory developed in this paper. The weak point of the proposed theory is the approximation of the cell membrane as an infinite rigid plane. The following arguments can be presented in support of this approximation.

The size of human cells is on the order of $10 - 100$ μm [16], while a representative diameter of currently used contrast agents lies in the range from about 1 to 3 μm. Also, one can see in Fig. 3, which was calculated for a contrast bubble with a diameter of 3 μm, that the diameter of the area where the maximum stress is reached and supposedly a hole emerges, is on the order of $1.5 - 2$ μm. Therefore a cell can generally be considered as a substantially bigger object than both a contrast bubble and the part of the cell membrane where the main interaction between the cell and the bubble takes place.

As regards the rigidity of a cell, the elastic modulus of cell membranes is estimated to be on the order of $10 - 1000$ MPa; for example, for the membrane of lymphocytes the elastic modulus is 80 MPa [17]. Such high values show that a cell is a rather rigid object.

These arguments justify the use of the model of a rigid wall for the cell membrane, at least as a first approximation. Nevertheless we would like to emphasize that the main reason of why we have to use this assumption is that at present there is no theory for an elastic wall that could be incorporated into our calculations. We hope that our work will stimulate studies on surmounting this shortcoming.

Acknowledgment

A.A.D. gratefully acknowledges the financial support from the le STUDIUM®, Institute for Advanced Studies (Orleans, France).

References

[1] Goldberg B.B., Raichlen J.S., Forsberg F., *Ultrasound Contrast Agents: Basic Principles and Clinical Applications* (Martin Dunitz, London, 2001).

[2] Klibanov A.L., "Microbubble contrast agents: Targeted ultrasound imaging and ultrasound-assisted drug-delivery applications", *Invest. Radiol*. 41, 354-362 (2006).

[3] Kaddur K., Palanchon P., Tranquart F., Pichon C., Bouakaz A., "Sonopermeabilization: Therapeutic alternative with ultrasound and microbubbles", *J. Radiol*. 88, 1777-1786 (2007).

[4] Deng C.X., Sieling F., Pan H., Cui J., "Ultrasound-induced cell membrane porosity", *Ultrasound Med. Biol*. 30, 519-526 (2004).

[5] van Wamel A., Kooiman K., Harteveld M., Emmer M., ten Cate F.J., Versluis M., de Jong N., "Vibrating microbubbles poking individual cells: Drug transfer into cells via sonoporation", *J. Control. Release* 112, 149-155 (2006).

[6] Yang F., Gu N., Chen D., Xi X., Zhang D., Li Y., Wu J., "Experimental study on cell self-sealing during sonoporation", *J. Control. Release* 131, 205-210 (2008).

[7] Nyborg W.L., "Acoustic streaming near a boundary", *J. Acoust. Soc. Am*. 30, 329-339 (1958).

[8] Rooney A., "Shear as a mechanism for sonically induced biological effects", *J. Acoust. Soc. Am*. 52, 1718-1724 (1972).

[9] Lewin P.A., Bjorno L., "Acoustically induced shear stresses in the vicinity of microbubbles in tissue", *J. Acoust. Soc. Am*. 71, 728-734 (1982).

[10] Wu J., "Theoretical study on shear stress generated by microstreaming surrounding contrast agents attached to living cells", *Ultrasound Med. Biol.* 28, 125-129 (2002).

[11] de Jong N., Cornet R., Lancee C.T., "Higher harmonics of vibrating gas-filled microspheres. Part one: simulations", *Ultrasonics* 32, 447-453 (1994).

[12] Wu J., Nyborg W.L., "Ultrasound, cavitation bubbles and their interaction with cells", *Adv. Drug. Deliv. Rev.* 60, 1103-1116 (2008).

[13] Doinikov A.A., Zhao S., Dayton P.A., "Modeling of the acoustic response from contrast agent microbubbles near a rigid wall", *Ultrasonics* 49, 195-201 (2009).

[14] Doinikov A.A., Haac J.F., Dayton P.A., "Modeling of nonlinear viscous stress in encapsulating shells of lipid-coated contrast agent microbubbles", *Ultrasonics* 49, 269-275 (2009).

[15] Naugolnykh K.A., Ostrovsky L.A., *Nonlinear wave processes in acoustics* (Cambridge University Press, Cambridge, 1998).

[16] Vander A.J., Sherman J.H., Luciano D.S., *Human Physiology* (McGraw-Hill, New York, 2001), p. 38.

[17] Glaser R., *Biophysics* (Springer-Verlag, Berlin, 2001), pp. 87–91.